Regenerative Therapy 21 (2022) 225–238

Contents lists available at ScienceDirect

Regenerative Therapy

journal homepage: http://www.elsevier.com/locate/reth

Original Article

Role of quercetin and rutin in enhancing the therapeutic potential of mesenchymal stem cells for cold induced burn wound

Fatima Irfan [a], Fatima Jameel [a], Irfan Khan [a], Rummana Aslam [b], Shaheen Faizi [c], Asmat Salim [a, *]

[a] Dr. Panjwani Center for Molecular Medicine and Drug Research, International Center for Chemical and Biological Sciences, University of Karachi, Karachi-75270, Pakistan
[b] Yale School of Medicine, New Haven, CT 06519, USA
[c] HEJ Research Institute of Chemistry, International Center for Chemical and Biological Sciences, University of Karachi, Karachi-75270, Pakistan

ARTICLE INFO

Article history:
Received 15 March 2022
Received in revised form
12 June 2022
Accepted 23 July 2022

Keywords:
Cold-induced burn wounds
Melia azedarach bioactive compounds
hUC-MSCs
Scratch assay
Wound healing

ABSTRACT

Introduction: Cold burn wounds differ in their pathophysiological spectrum as compared to other types of burn wounds. These wounds have prolonged devastating effects on the body including hypertrophic scars, contracture, and necrosis. Mesenchymal stem cells (MSCs) are considered promising candidates for the complete regeneration of burn wounds. However, transplanted MSCs face the challenge to survive under the harsh tissue conditions. Preconditioning of MSCs with bioactive compounds may enhance their survival and regenerative potential for use in clinical applications. Bioactive compounds of *Melia azedarach* are well known for their potential role in treating different types of skin wounds due to their anti-inflammatory, anti-viral, anti-cytotoxic, and anti-oxidative properties. This study aims to evaluate the synergistic effects of human umbilical cord derived MSCs (hUC-MSCs) after preconditioning them with bioactive compounds of *M. azedarach* (quercetin and rutin) for cold induced burn wounds.
Method: Human umbilical cord MSCs (hUC-MSCs) were characterized based on their specific cell surface markers and treated with 20 μM of quercetin or rutin. *In vitro* scratch assay was performed to measure cell migration and wound closure. *In vivo* cold burn wound model was developed via direct exposure of the dorsal rat skin to liquid nitrogen. hUC-MSCs were subcutaneously transplanted next day of burn wound induction and wound was examined at different time points corresponding to the wound healing phases (days 3, 7, and 14). The regenerative potential of preconditioned hUC-MSCs was assessed in different groups; control (treated only with hUC-MSCs), and treated groups (quercetin or rutin treated hUC-MSCs). Healing potential and wound closure were evaluated by histological, gene expression, and immunohistochemical analyses of the wound tissues before and after treatment.
Results: Scratch assay exhibited enhanced cell migration towards wound closure in the treated groups as compared to the control. Macroscopic examination of the wound revealed scab formation at day 14 in control, whereas scab was detached and the wound tissue was remarkably remodeled in the treated groups. Comparison between the treated groups showed that burn wound treated with quercetin significantly increased healing potential than the rutin treated MSCs. Histological findings showed enhanced regeneration of skin layers along with hair follicles in the quercetin group, while increased neovascularization was noted in both treatment groups. Gene profile of wound healing mediators illustrated significant upregulation of *IL-5, IL-4, GPX-7, TXNRD-2, PRDX, VEGF,* and *FGF* and down-regulation of inflammatory cytokines *IL-1β* and *IL-6*.

* Corresponding author. Dr. Panjwani Center for Molecular Medicine and Drug Research, International Center for Chemical and Biological Sciences, University of Karachi, Karachi-75270, Pakistan. Tel.: + (92-21) 99261671; Fax: + (92-21) 34819018-9.
E-mail addresses: famughal1@gmail.com (F. Irfan), fatimajameel43@gmail.com (F. Jameel), khan@iccs.edu (I. Khan), rummana.aslam@yale.edu (R. Aslam), shaheenfaizi@hotmail.com (S. Faizi), asmat.salim@iccs.edu (A. Salim).
Peer review under responsibility of the Japanese Society for Regenerative Medicine.

https://doi.org/10.1016/j.reth.2022.07.011

Conclusion: In conclusion, synergistic effect of hUC-MSCs and bioactive compounds of *M. azedarach* enhances wound healing by reducing the inflammation, mitigating oxidative stress and enhancing neovascularization. The study findings will aid in designing more effective treatment options for cold burn wounds.

1. Introduction

Skin functions as a bacterial, physical and chemical barrier to protect the body against harsh external environment. Any damage to the skin can be devastating and should be recovered efficiently. Skin possesses the ability to regenerate itself after any trauma, through mediated interactions between cells and healing mediators, which triggers healing mechanisms to restore damages [1]. Each layer of skin performs a specialized function; epidermis regulates body temperature, dermis maintains structural integrity and assists in sensation, and hypodermis provides mechanical protection and thermoregulation [2]. Increase in the number of burn wound injuries is a challenge for the healthcare system because of the failure to manage the condition in a timely and systematic way. Burn injuries are classified as first, second, third, and fourth degree burns, based on the depth of penetration of injury and extent of tissue destruction. First and second degree burns are superficial, while third and fourth degree burns are deep wounds [3]. In a clinical setting, diagnoses of burn patients are based on total body surface area (TBSA) affected with the wound. Minor burns are first or second degree wounds which cover less than 10% of TBSA and moderate burns are second degree wounds covering more than 10% of TBSA. Severe burn wounds indicate that 1% TBSA is affected with third degree wounds [4].

The etiology of burn wounds includes heat, radiation, UV rays and cold. The extent of skin damage from these causative agents depends upon the area and length of exposure. Skin has the capacity to adapt physiological changes according to the external conditions. However, extreme cold temperature restricts this capacity and causes devastating effects ranging from tissue injury to complete tissue loss which ultimately causes burn [5]. Tissue rewarming after cold injury results in blood clots, cyanosis, edema, ischemia, vascular damage, and compromises cell functions. Moreover, these wounds have prolonged devastating effects on the body including hypertrophic scars, contracture, and necrosis [6]. The process of wound healing starts with inflammation, leads to proliferation, and ends with restoration of tissue. In the dynamic process of wound healing, the paracrine secretions and interaction with other skin cell types create a complex microenvironment where multiple overlapping phases are involved [7]. Any divergence or disturbance in these phases may cause impaired wound healing with several other complications. Major complications that occur in the wound healing process include prolonged scar formation, extended oxidative stress and inflammation [8]. Wound monitoring is essentially required to determine the progression and integrity of the damaged tissue. Wound assessment over time can deliver a significant therapeutic insight for dynamic process of healing. It is much needed to understand the underlying pathophysiology of damaged skin tissue and its subsequent layers.

Treatment and management of burn wound injuries have complex pathophysiology. The treatment methods commonly used are symptomatic; comprises medications such as anti-inflammatory drugs, analgesics, and antibiotics. Skin grafting is an option that causes permanent closure of the wound, but it has certain limitations such as unavailability of donors and graft rejections [9]. Cell-based therapy offers an unprecedented approach for developing treatment methods for burn wounds. Stem cells have potential to differentiate into multiple lineages. They migrate to the injury site in response to the signaling cascade. Pre-clinical data of umbilical cord derived MSCs shows their regenerative effect both locally and systemically. Local transplantation of MSCs at burn site resulted in downregulation of inflammatory genes and upregulation of proliferative genes having essential role in healing [10]. However, use of MSCs in clinical application is a challenge because of cellular senescence that results in reduction of cell number after an *in vivo* transplantation [11].

The screening and extraction of biologically active components of plants have improved treatment strategies and drug development. Some plants are considered as potent wound healers for having anti-inflammatory, anti-coagulant, and anti-oxidant properties [12]. Medicinal plants were used in traditional medicine for many years; 25% of the active drug components are obtained from plant sources [13]. Plant extracts were tested and verified to have therapeutic potential for treating different types of wound infections. The wound healing efficacy of *Melia azedarach* has long been ignored in the modern medicine. *M. azedarach* has anti-inflammatory, anti-microbial, cytotoxic, and anti-viral activities which can be beneficial for the wound healing process [14]. Major active components of *M. azedarach* include terpenes, steroids, flavonoids, proteins, saponins, alkaloids, phytosterols, and phenols. The two flavonoids of *M. azedarach* i.e., quercetin and rutin possess potent anti-inflammatory and anti-oxidant properties necessary for efficient wound healing [15,16].

This study was designed to utilize the wound healing properties of *M. azedarach* compounds, quercetin and rutin, and evaluate their synergistic role with human umbilical cord derived MSCs (hUC-MSCs) in both *in vitro* and in the *in vivo* wound models via pre-conditioning approach.

2. Material and methods

2.1. Materials/reagents

The reagents used in the study are as follows: Alexa fluor 546 goat anti-mouse secondary antibody, Alpha smooth muscle actin, α-SMA (Invitrogen, USA), Bovine serum albumin (BSA), CD45 (BD Bioscience, USA), CD90 (Cederlane International, Canada), CD177 (Zymed Laboratories), DAPI, Tween 20 (MP Biomedicals, USA), DiI dye (Life Technologies Corporation, USA), DPX mounting medium (Merck, Millipore, USA), Dulbecco's Modified Eagle's Medium (DMEM), Fetal bovine serum (FBS), Hematoxylin & Eosin (H & E) stain kit (Carl-ROTH, Germany), Fluoromount-aqueous mounting media, MTT, Ketamine hydrochloride, Vimentin, Xylazine (Sigma Aldrich, USA), Optimal cutting temperature (OCT) medium (Tissue Tek, USA), RevertAid First Strand cDNA synthesis kit, SYBR Green/ROX qPCR Master Mix (Thermo Fisher Scientific, USA), Sodium pyruvate, Streptomycin/penicillin, Trypsin (Gibco, USA).

2.2. Ethical approval

The study was approved by the local Independent Ethical Committee (IEC) and Institutional Animal Care and Use Committee (IACUC); IEC/ICCBS-036-HT-2018/Protocol/1.0 and Animal study protocol (ASP) number 2021–008, respectively. Umbilical cord samples were obtained from Zainab Panjwani Memorial Hospital after a caesarean delivery following informed consent from the donor parents. Male Wistar rats (180–250 gm) were obtained from institutional Animal Research Facility (ARF) and housed at 12 h light: dark cycle, 25± 1 °C temperature and 55 ± 5% humidity.

2.3. Isolation and culture of hUC-MSCs

Each cord sample (6–8 cm) was collected in sterile 1X phosphate buffered saline (PBS) and 0.5% EDTA, and stored at 4 °C until further processing. The sample was processed in a Biosafety Cabinet-II (ESCO, USA) within 3 h after collection using protocol described in our previous study [17]. Briefly, cord was washed with 1X PBS to remove blood clots and cut into 2–3 mm pieces to expose Wharton's jelly. After 10–15 days, MSCs adhered to the flask with their typical morphological characteristics. When cells reached 70–80% confluence, they were re-plated by separating the adherent confluent monolayer of cells by adding 1X trypsin. Floating cells were centrifuged at 1000 rpm for 8 min and pellet was resuspended in media to sub-culture the cells. Cells were supplemented with DMEM, 10% FBS, 100 units/mL penicillin and 100 μg/mL streptomycin. Media was changed after every two to three days, and cells were incubated at 37 °C and 5% CO_2. All experiments were conducted using cell passages P2 and P3.

2.4. hUC-MSC characterization by immunocytochemistry

Immunocytochemistry was performed to characterize the cells on the basis of their specific cell surface markers. Approximately, 10,000 cells were seeded in 24 well plate and placed in an incubator at 37 °C for 24 h. When the cells formed a monolayer, medium was removed and wells were washed twice with 1X PBS. 200 μL of 4% paraformaldehyde (PFA) was added for cell fixation followed by 10 min incubation. Cells were permeabilized for 10 min by treatment with 0.1% Triton X-100 and then 200 μL blocking solution (2% BSA and 0.1% Tween 20) was added to block non-specific binding sites. After 1 h, blocking solution was aspirated out and primary antibodies CD90, CD117 and vimentin (positive markers), or CD45 (negative marker) were added at recommended dilutions and incubated for 24 h at 4 °C. Alexa flour 546 secondary antibody solution was added at a dilution of 1:200 along with F-actin (1:200) in the blocking solution for 1 h followed by 15 min incubation with DAPI (0.5 μg/mL) at 37 °C. Cells were observed under fluorescence microscope (Eclipse Ni-E, Nikon, Japan) after mounting the slides with DPX mounting medium.

2.5. Preconditioning of hUC-MSCs with quercetin and rutin

The bioactive compounds of *M. azedarach,* quercetin and rutin were provided by Prof. Dr. Shaheen Faizi, HEJ, International Center for Chemical and Biological Sciences, University of Karachi. Cytotoxic concentration of each compound was calculated by performing MTT assay using manufacturer's guidelines. Different concentrations of the compounds were used ranging from 5 μM to 100 μM for treatment with hUC-MSCs and incubated for 24 h under standard culture conditions. Concentration of 20 μM was selected for preconditioning of hUC-MSCs for further experiments. These compounds will be referred to Q (quercetin) and R (rutin) in the subsequent sections.

2.6. Scratch assay

Cell migration was analyzed by scratch assay. Physical exclusion method was employed to create a cell free gap with the help of 20 μL sterile pipette tip. Scratch reproducibility was maintained by controlling the pressure and angle of the pipette. The experiment comprised of three replicates of each group i.e., hUC-MSCs, Q + hUC-MSCs and R + hUC-MSCs. Optimized concentration (20 μM) of each compound was added to the flask for 24 h. The experiment was monitored at respective time points (0 h–48 h) under phase contrast microscope (TE 2000S Eclipse, Nikon, Japan). Cell migration was calculated by measuring the distance covered to fill cell gap (scratch).

2.7. In vivo *experimental design*

The study is divided into four experimental groups: Control (no treatment), and treatment groups of hUC-MSCs, Q + hUC-MSCs and R + hUC-MSCs. Macroscopic analysis, histopathology, immunohistochemistry and gene expression analysis of the wound tissues were performed on three respective wound healing time points (days 3, 7 and 14). Total 53 animals were used in the study and each experiment was performed in triplicate.

2.8. Cold burn wound model

Prior to wound induction, the animals were anesthetized with xylazine (7 mg/kg) and ketamine hydrochloride (60 mg/kg). Hairs were removed from the dorsal surface and skin was disinfected with the alcohol swab. Steel rod (1.5 cm diameter and 198 gm weight) was dipped in liquid nitrogen for 20 min, and placed on the dorsal surface for 25 s. Analgesic (diclofenac sodium) and antibiotics (penicillin/streptomycin) were given to the animals after wound induction.

Table 1
Targeted genes with their primer sequences and annealing temperature.

Gene	Primer Sequences (5′-3′)	Annealing Temperature (°C)
Interleukin 1 beta (IL-1β)	F: TCATCTTTGAAGAAGAGCCCGT R: TCATCTTTGAAGAAGAGCCCGT	58
Interleukin 6 (IL-6)	F: GATGGATGCTTCCAAACTGGATA R: TGAATGACTCTGGCTTTGTCTTT	58
Interleukin 4 (IL-4)	F: CGTGATGTACCTCCGTGCTT R: ATTCACGGTGCAGCTTCTCA	58
Interleukin 5 (IL-5)	F: TGATACAGCTGTCCACTCACC R: TGCCCACTCTGTACTCATCAC	58
Glutathione peroxidase 7 (GPX7)	F: AGGAGATCAAGCCCCGTAT R: CGAAGGGAAGAGAAGCATT	58
Peroxiredoxin 7 (PRDX7)	F: CAAAGCCACGGCTGTTATGC R: TGGGTCCCAATCCTCCTTGT	58
Thioredoxin reductase 2 (TXNRD2)	F: GCCCAGTACAAGGCTCTCA R: AGGTTAGAGGGGGCAGTCA	58
Vascular endothelial growth factor (VEGF)	F: TGAATGACTCTGGCTTTGTCTTT R: TGAATGACTCTGGCTTTGTCTTT	58
Fibroblast growth factor (FGF)	F: AGCAGAAGAGAGAGGAGTTGTG R: TATTTCCGTGACCGGTAAGTGT	58
Glyceraldehyde-3-phosphate dehydrogenase (GAPDH)	F: GGAAAGCTGTGGCGTGATGG R: GTAGGCCATGAGGTCCACCA	58
F = forward primer, R = reverse primer		

2.9. Transplantation of normal and preconditioned hUC-MSCs

Approximately, 1 million cells were used for transplantation after 24 h of wound induction. After trypsinization, the pellet was washed and resuspended in 300 μL 1 X PBS. The cells were transplanted subcutaneously around wound peripheries at multiple injection sites. Tissues were harvested at respective time points i.e. days 3, 7 and 14 after euthanizing the animal.

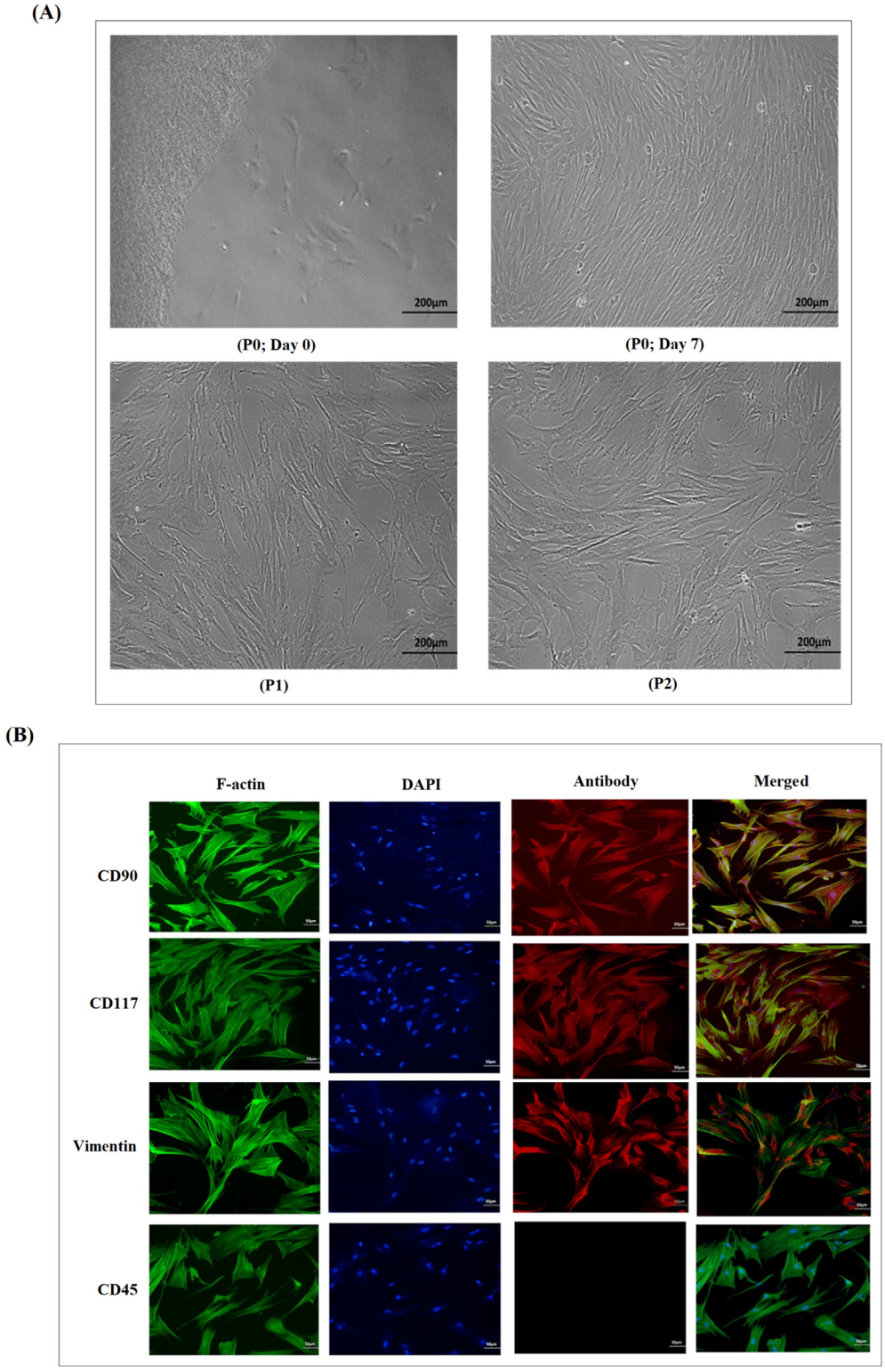

Fig. 1. Morphology and Characterization of hUC-MSCs (A) hUC-MSCs extended from explants at day 0, and reached 70–80% confluence after 7 days in culture. hUC-MSCs showed fibroblast-like morphology at passage 1 (P1) and passage 2 (P2). Images were taken under phase contrast at 10× magnification (B) Positive expression of hUC-MSC specific markers CD90, CD117, vimentin, and negative expression of CD45 (a hematopoietic marker) was observed. F-actin staining shows the cytoskeleton and DAPI staining represents nuclei of hUC-MSCs. Images were taken under fluorescence at 20× magnification.

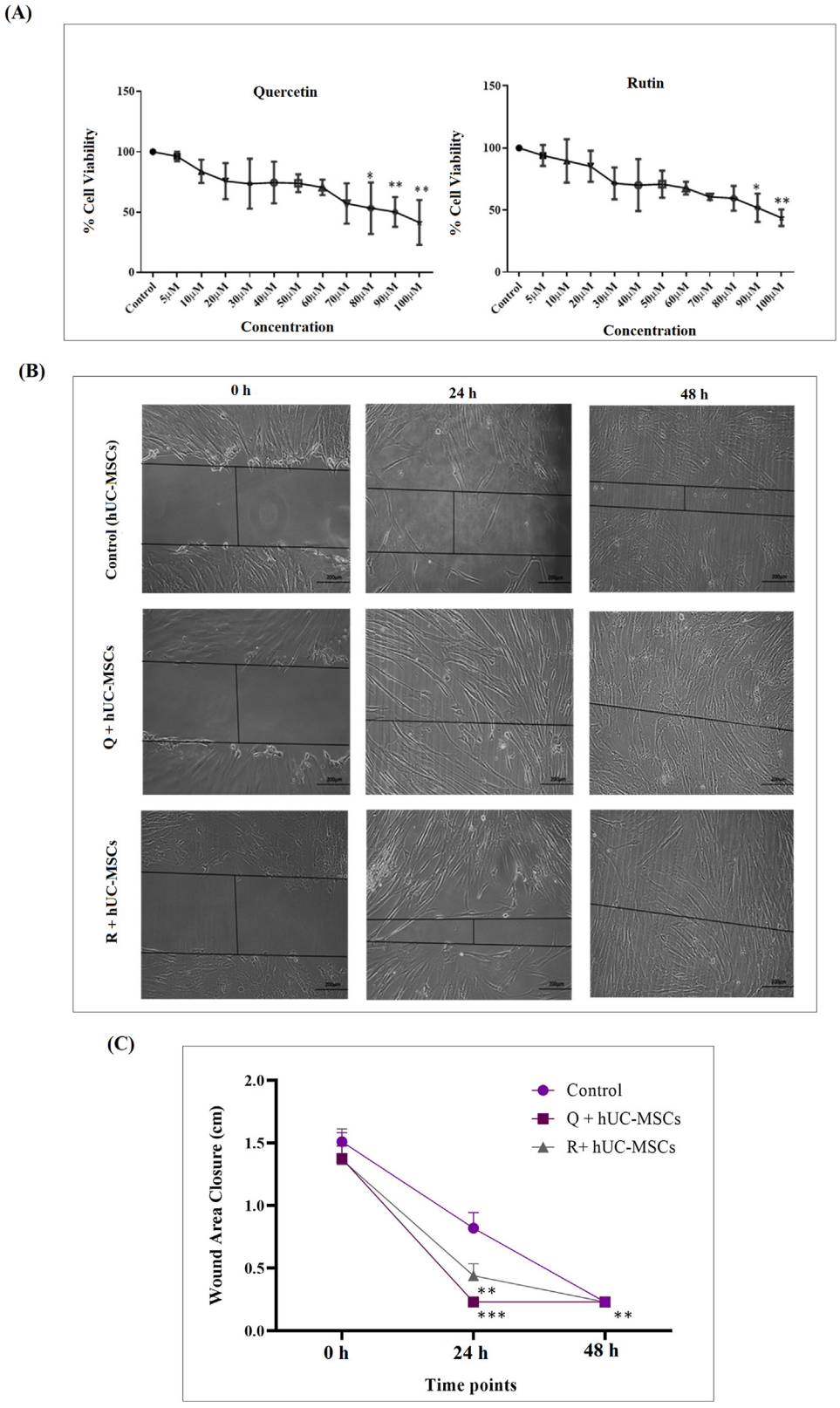

Fig. 2. Cytotoxicity analysis and *in vitro* wound healing assay (A) Non-cytotoxic concentration of compounds (quercetin and rutin) was determined using MTT assay. The cell viability decreased in a concentration dependent manner. For statistical analysis, one-way ANOVA with Bonferroni post-hoc test was performed. Data is represented as mean ± S.E.M (n = 3); p-value ≤ 0.05 was considered statistically significant (where ** = $p < 0.01$, * = $p < 0.05$) (B) Phase contrast images of 0 h, 24 h and 48 h of scratch assay with hUC-MSCs, quercetin treated MSCs (Q + hUC-MSCs) and rutin treated MSCs (R + hU-MSCs). Significant reduction in scratch area was observed in the treated groups as compared to control. Wound healed at 24 h in quercetin and 48 h in rutin treated groups (C) Graphical illustration of percentage wound area closure showed considerable reduction in scratch area in treated groups as compared to control. For statistical analysis, one-way ANOVA with Bonferroni post-hoc test was performed. Data is represented as mean ± S.E.M (n = 3); p-value ≤ 0.05 was considered statistically significant (where *** = $p < 0.001$, ** = $p < 0.01$).

2.10. Homing of normal and preconditioned hUC-MSCs

Cell homing at the wound site was analyzed by tracking the cells with 5 μM DiI dye. Cell pellet was washed with 1 X PBS followed by 7 min incubation with the dye, then washing again with 1 X PBS. Labeled cells were transplanted subcutaneously and tissue was harvested at day 14. Tissue was fixed in 4% PFA for 4 h and placed in a tissue mold with OCT for embedding. Tissue was frozen and sections of 10 μm were cut using cryostat (Shandon Cryotome E). Sections were stained using DAPI (0.5 μg/mL) and mounted using fluoromount-aqueous mounting media. Stained sections were observed under fluorescence microscope.

2.11. Macroscopic evaluation

Skin wound tissues of all groups (control and treated hUC-MSCs) were visualized for signs of scab formation, granulations, inflammation and wound contraction. Images were taken at respective time points at days 3, 7 and 14, and compared. Wound closure was measured as per the protocol defined in a previous study using the formula: area of actual wound (S1)/area of original wound (S0) [18].

2.12. Histological evaluation

Harvested tissues of all groups were fixed in 4% PFA (overnight incubation), followed by serial dehydration steps. Tissue samples were embedded with paraffin and sections of 6 μm were cut and mounted on gelatin coated slides. Sections were stained using Hematoxylin & Eosin (H & E) as per the guidelines of the manufacturer.

2.13. Immunohistochemical analysis

Neo-vascularization in the burn wound tissue was analyzed at day 14 with immunohistochemistry using α-smooth muscle actin (α-SMA) antibody. The sections were deparaffinized and antigen retrieval was performed by exposing the tissues with sodium citrate buffer for 45 min at 90-100 °C. Blocking solution was added to the slides to prevent non-specific binding. α-SMA solution (1:100) was added to the slides and incubated overnight at 4 °C. Next day, Alexa fluor 488 secondary antibody (1:200) was added after washing the slides with PBS-tween 20 buffer. After 2 h incubation, DAPI (0.5 μg/mL) was added for 10 min. Tissue sections were

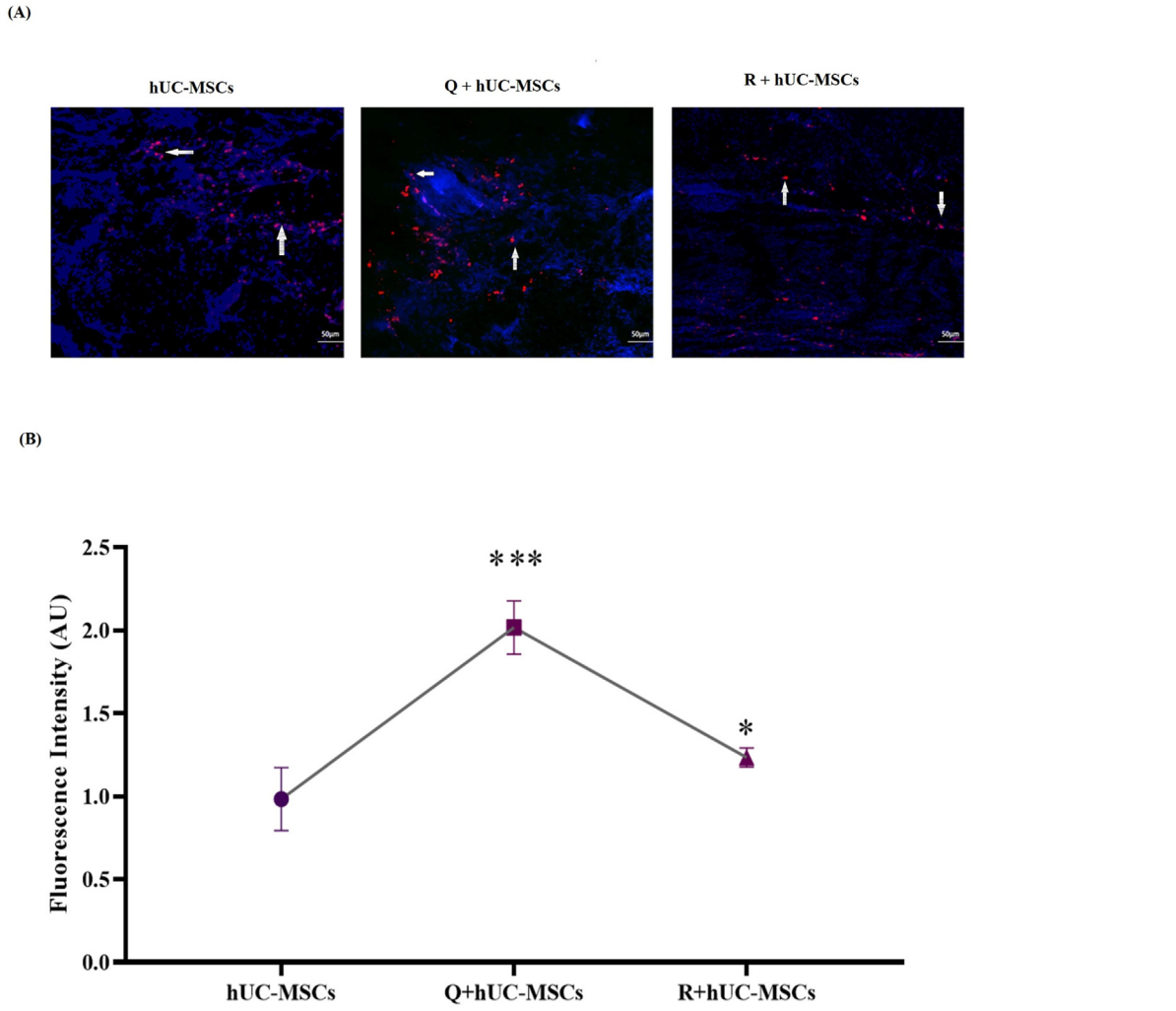

Fig. 3. Cell homing at the wound site (A) Tracking of hUC-MSCs was performed at day 14. DiI labeled red fluorescent cells representing hUC-MSCs were observed around the center of wound lesion. Some labeled cells are indicated with white arrows (B) Quantitative analysis of labeled cells represent significant increase in the fluorescence intensity in the treated groups as compared to untreated control. Statistical analysis was performed using one-way ANOVA with Bonferroni post-hoc test. Data is represented as mean ± S.E.M ($n = 3$); p-value ≤ 0.05 was considered statistically significant (where *** = $p < 0.001$, * = $p < 0.05$).

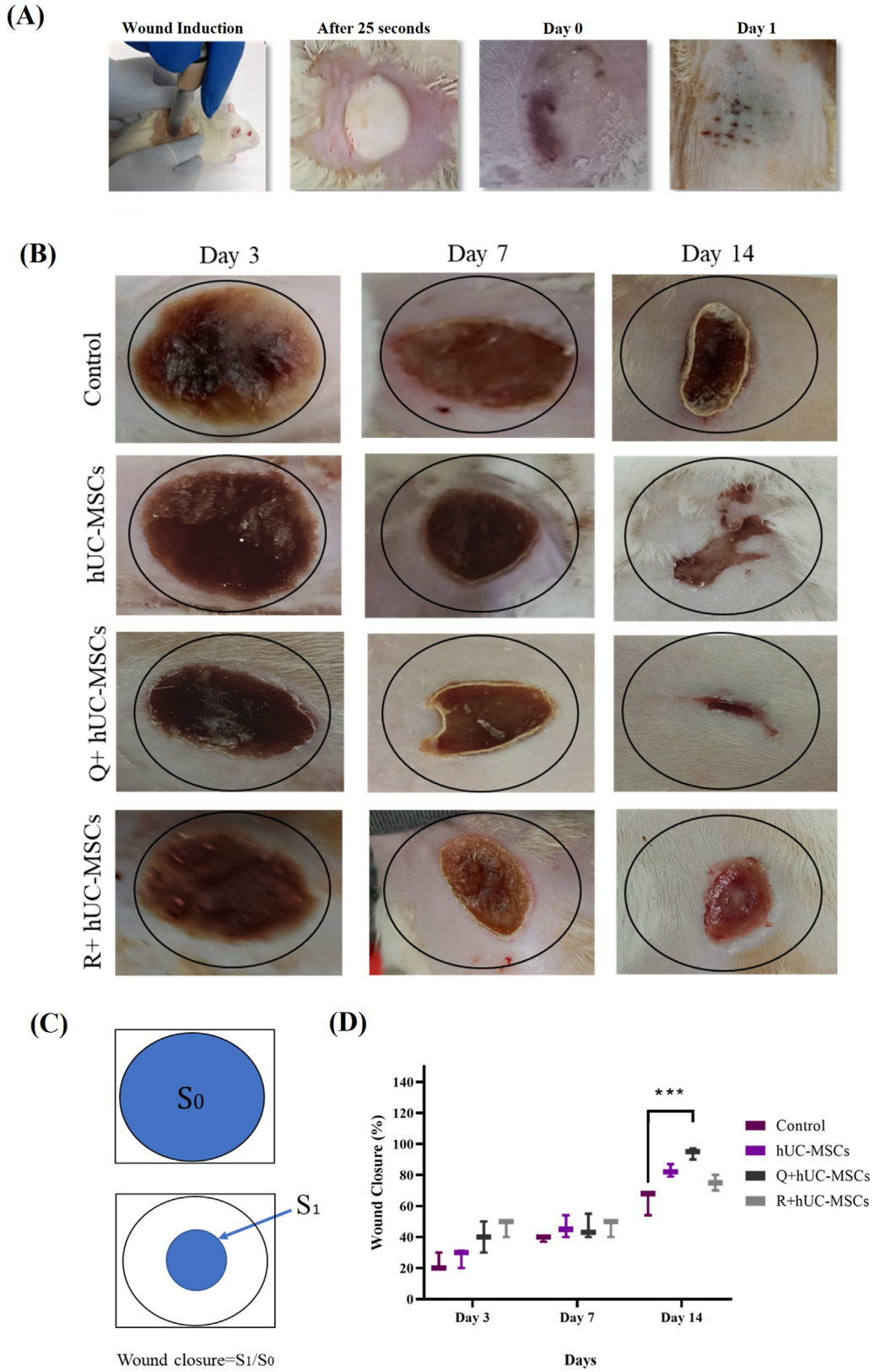

Fig. 4. Macroscopic evaluation of cold burn wound (A) Immediately after the burn wound induction, wound area showed freezing of the skin. At day 1, black eschar formation was prominent (B) Images representing macroscopic changes of the cold burn wounds including the general appearance, the size of the wound, time for tissue granulation and the hair regeneration at respective wound healing phases. At day 3, edema and necrosis were observed in the control group, whereas Q + hUC-MSCs represented wound surrounded with a fine crust layer. The scab was prominent at day 7 in treatment groups, while in the control group, it appeared at day 14. In the treatment groups, scab was detached at day 14 and wound appeared to be contracted (C) Images showing schematic representation of the wound closure and formula used for analysis (D) Graphical illustration representing wound closure in all groups with statistically significant reduction in wound closure in the Q + hUC-MSC group. One-way ANOVA with Bonferroni post-hoc test was performed for statistical analysis. Data is represented as mean ± S.E.M (n = 3); p-value ≤ 0.05 was considered statistically significant (where *** = $p < 0.001$).

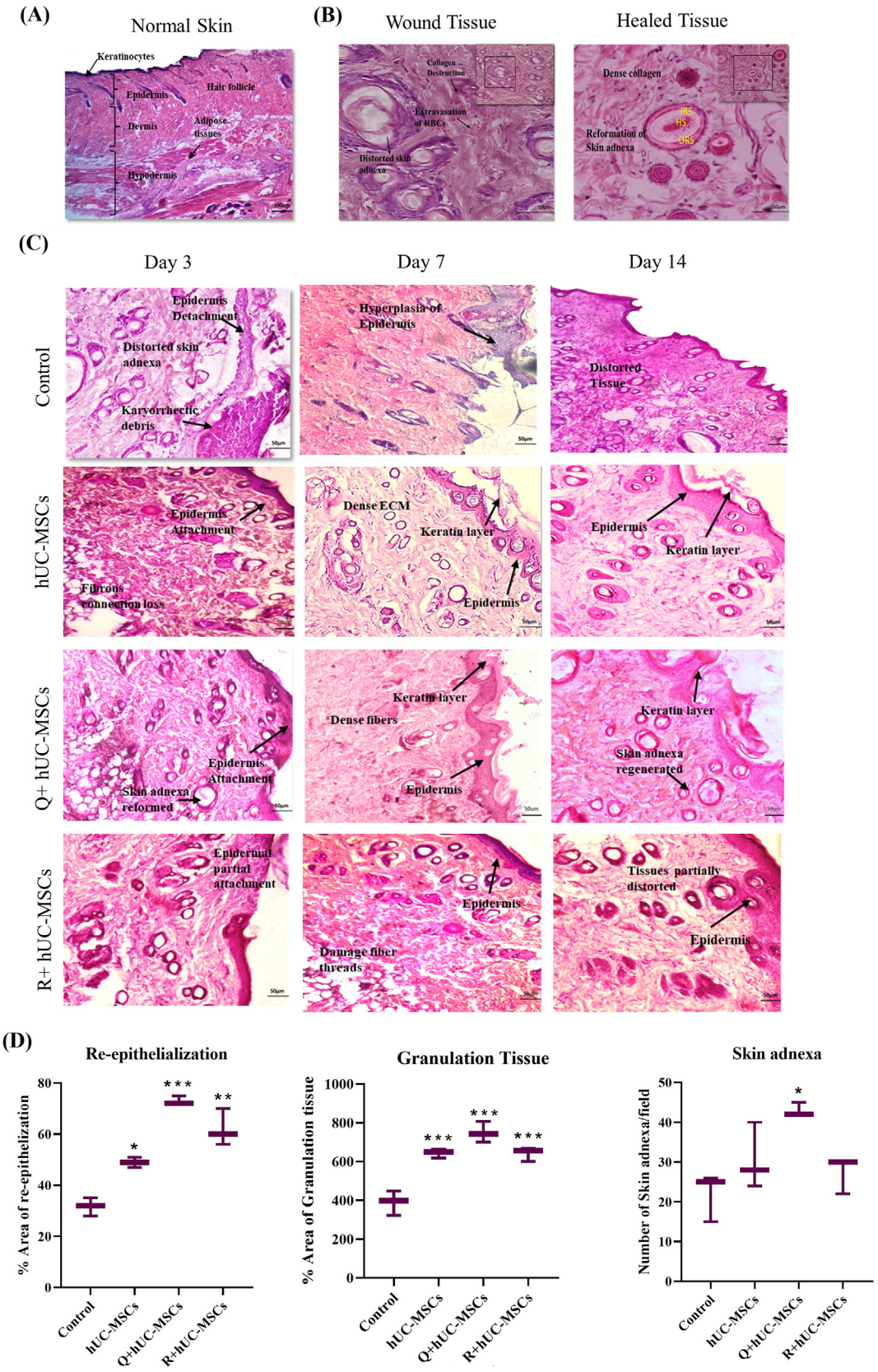

Fig. 5. Histological evaluation of the cold burn wound model and treatment groups (A) Histology of the normal skin featuring all skin layers; epidermis, dermis, hypodermis and thick keratinocytes along with hair follicles (B) Skin adnexa were observed in the wound and healed tissues. In the wound tissue, skin adnexa were distorted, surrounded with inflammatory cells and extravasation of RBCs, however in the healed tissue, there was a specified morphology with HS (hair shaft), IRS (inner root sheath), and ORS (outer root sheath) (C) Comparative histology of all experimental groups at respective time points ie. days 3, 7 and 14. Prominent features are as follows: At day 3: Control: distorted skin adnexa, karryohectic debris, epidermis detachment; hUC-MSCs: tissue distortion, epidermis and dermis attached; Q + hUC-MSCs: skin adnexa started to repair, re-epithelialization;

observed under fluorescence microscope after mounting the slides with DPX mounting medium.

2.14. Gene expression analysis

Harvested tissues were pulverized, homogenized, and sonicated to isolate RNA using one step RNA reagent using manufacturer's protocol. RNA quantification was performed at 260 nm using spectrophotometer (UV-1700, Shimadzu, USA). Volume of RNA corresponding to 1 μg concentration was used for the synthesis of cDNA using manufacturer's protocol. The amplification and analysis of genes representing wound cytokines (Table 1) at different phases of healing was performed through qPCR. GAPDH gene was amplified along with the targeted genes as the experimental control.

2.15. Statistical analysis

Statistical analysis was performed using IBM SPSS software 21 and GraphPad Prism 8. Group comparison was performed using one-way ANOVA and Bonferroni post-hoc test. Data is presented as mean ± SEM and $p < 0.05$ was considered as statistically significant (* = $p \leq 0.05$, ** = $p \leq 0.01$ and *** = $p \leq 0.001$).

3. Results

3.1. Characterization of hUC-MSCs

The cells initially represented a heterogeneous population when isolated from human umbilical cord and then within a week, they showed homogenous morphology. After 10 days of isolation, the cells adhered to the flask surface and within 12 days reached 70–80% confluence. hUC-MSCs were identified based on their fibroblast like morphology (Fig. 1A). Cells were passaged to P1 and then P2 when they reached 70% confluence. Immunocytochemical characterization of hUC-MSCs showed strong expression for CD90, CD117 and vimentin (Fig. 1B). These markers are specific for MSCs. The cells showed negative expression of CD45, which is a hematopoietic marker.

3.2. Cytotoxicity analysis of quercetin and rutin

Cell cytotoxicity increased with increased concentration of both compounds, quercetin and rutin. In case of quercetin, number of apoptotic cells increased at concentrations of 80 μM and above, while in case of rutin, 90 μM and above concentration were cytotoxic to cells. Non-cytotoxic concentration of 20 μM was selected for both compounds to precondition hUC-MSCs in separate groups (Fig. 2A).

3.3. In vitro wound healing analysis via scratch assay

Wound healing potential of quercetin and rutin treated hUC-MSCs was analyzed with scratch assay. The assay showed complete closure of the scratch at 24 h and 48 h in the quercetin and rutin treated MSCs, respectively (Fig. 2B). Statistical analysis showed significant reduction in the scratch area in both quercetin and rutin treated groups as compared to untreated control (Fig. 2C).

3.4. Homing of hUC-MSCs at the wound site

The increased expression of DiI labeled cells was observed in quercetin and rutin treated hUC-MSCs as compared to untreated hUC-MSCs indicating that cell survival was enhanced after treatment (Fig. 3A and B).

3.5. Gross macroscopic wound analysis and wound closure assessment

The healing pattern was observed after induction of cold burn wound at different time points. Immediately after wound induction, burn area was contracted and frozen due to the exposure to the chilled rod (Fig. 4A). After day 1 of wound induction, severe edema was observed, resulting in uniform black eschar formation. Black dotted blisters were also observed at the surface of the wound (Fig. 4A). Comparative macroscopic wound closure analysis of all groups was performed based on inflammation, crust, color of lesion, re-epithelization, time of wound closure and granulation at days 3, 7 and 14 as shown in Fig. 4B. At day 3, inflammation was dominant and the lesion showed blackening of the burn area around the wound in the untreated and both the treated groups. In case of Q + hUC-MSC group, entire area of the burn wound was covered with a solid narcosis layer by day 3. At day 7, a small crust formation was observed around the wound edges and demarcation started to appear along with persistent skin inflammation in the control group. In the treated groups, prominent scab formation occurred especially in the Q + hUC-MSC group. The crust turned dry, and shrinkage of wound edges was noted. At day 14, similar macroscopic features were observed in the control group that appeared at day 7 in Q + hUC-MSC group indicating the formation of tissue granulation. At day 14, hUC-MSC, Q + hUC-MSC and R + hUC-MSC groups showed scab detachment by forming a new second discreet crust. Statistical analysis performed by measuring wound closure showed significant wound contraction at day 14 in the Q + hUC-MSC group as compared to control (Fig. 4C and D).

3.6. Microscopic analysis of burn wound tissues

3.6.1. Histopathological analysis

Histopathological evaluation of the wound tissues at different time points supported our macroscopic analysis. Patterns of normal skin and wound healing phases are presented in Fig. 5. Normal skin showed clear demarcations of all three skin layers i.e., epidermis, dermis and hypodermis. Thick keratinocyte layer was evident above the epidermis. Hair follicles extended from epidermis to dermis. Dermis showed compact tissue structure and hypodermis represented well defined adipose tissues. All the features clearly validate the histology of normal skin (Fig. 5A). The analysis of histopathology of the wound tissue revealed damaged skin adnexa, which is a specialized structure located in the dermis consisting of hair follicles, apocrine gland, and sebaceous glands. Healed tissue represents formation of new dense extracellular network, recovery of skin appendages, and the internal layers of hair follicles including hair shaft, inner root sheath and outer root sheath (Fig. 5B). In case of the wound tissue, not only the layers were affected but the internal components were also damaged due to the burn injury (Fig. 5C). At day 3, the tissue morphology represented

R + hUC-MSCs: partial re-epithelialization. At day 7: Control: hyperplasia of epidermis; hUC-MSCs: re-epithelization, distorted ECM, keratin layer; Q + hUC-MSCs: compact dense fibrous connections; R + hUC-MSCs: partial tissue distortion. At day 14: Control: re-epithelization, tissue distortion; hUC-MSCs: dense fibrous connections, epidermal and dermal attachment; Q + hUC-MSCs: reformed skin adnexa, dense ECM, thick keratin layer, re-epithelization; R + hUC-MSCs: re-epithelization, dense ECM (D) Statistical analysis representing enhanced re-epithelization and granulation at day 14 in all treatment groups, and increased number of skin adnexa per field in Q + hUC-MSC group as compared to control. One-way ANOVA with Bonferroni post-hoc test was performed. Data is represented as mean ± S.E.M (n = 3); p-value ≤ 0.05 was considered statistically significant (where *** = $p < 0.001$, ** = $p < 0.01$, * = $p < 0.05$).

disturbance of overall tissue integrity as skin layers were not distinguishable with loss of extracellular matrix connection in all experimental groups. In the control group, accumulated karyorrhectic debris were observed at day 3 as a result of fragmentation of keratinocytes and other skin layers damaged during inflammation. Furthermore, at day 3, Q + hUC-MSC group showed attachment of basement membrane, while R + hUC-MSC group showed partial attachment of epidermal layer. At day 7, epidermis started to regenerate with multiple types of cells including squamous epithelium, keratinocytes and melanocytes. Extracellular matrix connection became dense in Q + hUC-MSCs treated group whereas it was still distorted in R + hUC-MSCs as compared to control. At day 14, histopathology represented the remodeling phases via migration of skin cells as tissue has no distortion and compact structure of dermis was reformed. At this stage, treated tissue showed superficial layer reformation indicated by thick covering of keratinocytes, while epidermis was completely regenerated and dermis was filled with moderate number of fibroblasts and blood vessels (Fig. 5C). In treated tissues, the reparative characteristics of skin layers were further analyzed. Quantification of histology revealed statistical significance in area of re-epithelization and granulation at all treatment groups at day 14. Number of skin adnexa per field was significantly increased at day 14 in the Q + hUC-MSC group as compared to control (Fig. 5D).

3.6.2. Analysis of neo-vascularization

Blood vessels were identified and quantified in the tissue sections by α-SMA immunostaining at day 14. The treated tissues showed increased number of blood vessels as compared to control (Fig. 6A). Statistical analysis showed significant increase in the number of blood vessels in all treatment groups with highest number in the Q + hUC-MSC group (Fig. 6B).

3.7. Gene expression analysis

Time dependent changes in the gene expression pattern were observed in all experimental groups. Inflammatory cytokines IL-1β and IL-6 showed downregulation in the treatment groups. IL-1β was downregulated at days 7 and 14 in the hUC-MSC group, and at all-time points in Q + hUC-MSC and R + hUC-MSC groups (Fig. 7A). Significant downregulation of IL-6 at days 7 and 14 was observed in all treatment groups (Fig. 7B). Anti-inflammatory genes IL-5 and IL-4 were upregulated in Q + hUC-MSC group at day 3 (Fig. 7C and D). Oxidative stress induced genes, GPX-7 and PRDX-7 showed significant upregulation in the R + hUC-MSC group at days 3 and 7, respectively, whereas TXNRD-2 was significantly upregulated at day 3 in case of Q + hUC-MSCs (Fig. 7E–G). Genes responsible for cell proliferation, VEGF and FGF were significantly upregulated in the treatment groups at different time points compared to control. R + hUC-MSCs showed increased VEGF expression at days 7 and 14, while Q + hUC-MSCs showed upregulation of both VEGF and FGF at day 14 (Fig. 7H, I).

4. Discussion

Despite the availability of various reconstructive therapeutic options, the complete covering of soft wound tissues is still a difficult and challenging procedure, especially when it is associated with fractures and deep burn wounds. Artificial skin grafting is a commonly performed procedure, however, it offers poor functionality of skin and cosmetic outcomes [9]. In case of allogenic skin grafting, several cases of immune rejection or graft versus host disease are reported, which need necessary immunosuppressive treatment [19]. The major hurdle to successful skin engraftment is the incorporation of functional vasculature to provide essential nutrients and oxygen supply at the wound site. However, the use of biomaterials in the field of tissue engineering has driven the rapid development of vascularized skin tissue production, leading to new technologies such as 3D bio-printing and nano-fabrication of scaffolds. Stem cells have gained interest as a better therapeutic option due to their self-renewal and plasticity properties as high regeneration potential, that contributes significantly to the efficient wound healing process [20]. The existing data from preclinical studies suggests that stem cell therapy aids in reducing burn wound area significantly, thus providing useful insight for future clinical studies for burn wound management [21]. In addition, they can be potentially used to treat skin wounds due to their less immunogenic property [22].

Preconditioning of stem cells can aid in increasing their regenerative potential by treating them with bioactive chemical compounds. This is a promising strategy to enhance the wound healing process. Preconditioning can aid stem cells to adapt to the pathological environment by stimulating protective and cell survival pathways [23]. In this study, we analyzed the effect of two bioactive compounds of *M. azedarach*, quercetin and rutin, in enhancing the potential of hUC-MSCs for rat cold burn wound model. Rat cold burn wound model was developed and characterized via the appearance of prominent black eschar around the wound edges indicating second degree burn as reported in a previous study [24]. MSCs migrate and home to the wound site due to the chemotactic response generated by the wound microenvironment [25,26]. However, transplanted MSCs face the challenge to survive under the harsh tissue conditions. We hypothesized that preconditioning of hUC-MSCs after treatment with the two bioactive compounds can promote wound healing due to their cytoprotective properties. hUC-MSCs were successfully isolated and characterized based on their specific cell surface markers and treated with non-cytotoxic concentrations of rutin or quercetin. The results indicated that treated hUC-MSCs promoted wound closure in both the monolayer cultures as well as in the animal model. Our previous study reported that transplantation of hUC-MSCs at the wound site leads to scar less healing because of the attenuated inflammatory response and increased cell proliferation [17]. Macroscopic results were further correlated with those of scratch assay that showed improved cell migration by quercetin and rutin treatment.

Macroscopic and microscopic evaluation of the wound tissues and their comparative analyses with normal skin showed extensive destruction of the injured skin. Wound maturation is the foremost feature analyzed via histopathology with regeneration of blood vessels, ECM remodeling and reformation of skin layers. In a previous study, transplantation of hUC-MSCs at the wound site resulted in their enhanced regeneration potential by regulation of cell signaling related healing cascade [27]. In our study, wound tissues showed characteristic morphology such as, detachment of epidermis, distortion of skin adnexa, disorganization of extracellular matrix and formation of karyorrhectic debris. The most important feature observed at the inflammation phase of cold burn wound was the degradation of skin appendages in the form skin adnexa. Damage to the skin adnexa is considered as deep dermal damage which results in progressive skin inflammation [28]. Besides, red blood cells were also observed due to the extravasation or blood vessel destruction. Comparative analysis of the treatment groups showed that wound closure was significantly enhanced in Q + hUC-MSCs group. Quercetin is known to reduce duration of the wound healing phases and enhance wound closure by increasing the epithelial cell growth [29]. We observed scab formation at day 14 in the control group, whereas it was prominent at day 7 in all treatment groups. Scab formation can protect the underneath tissue from hemorrhage and allows healing to occur at the surface [24]. At day 14, re-epithelialization was observed in the Q + hUC-

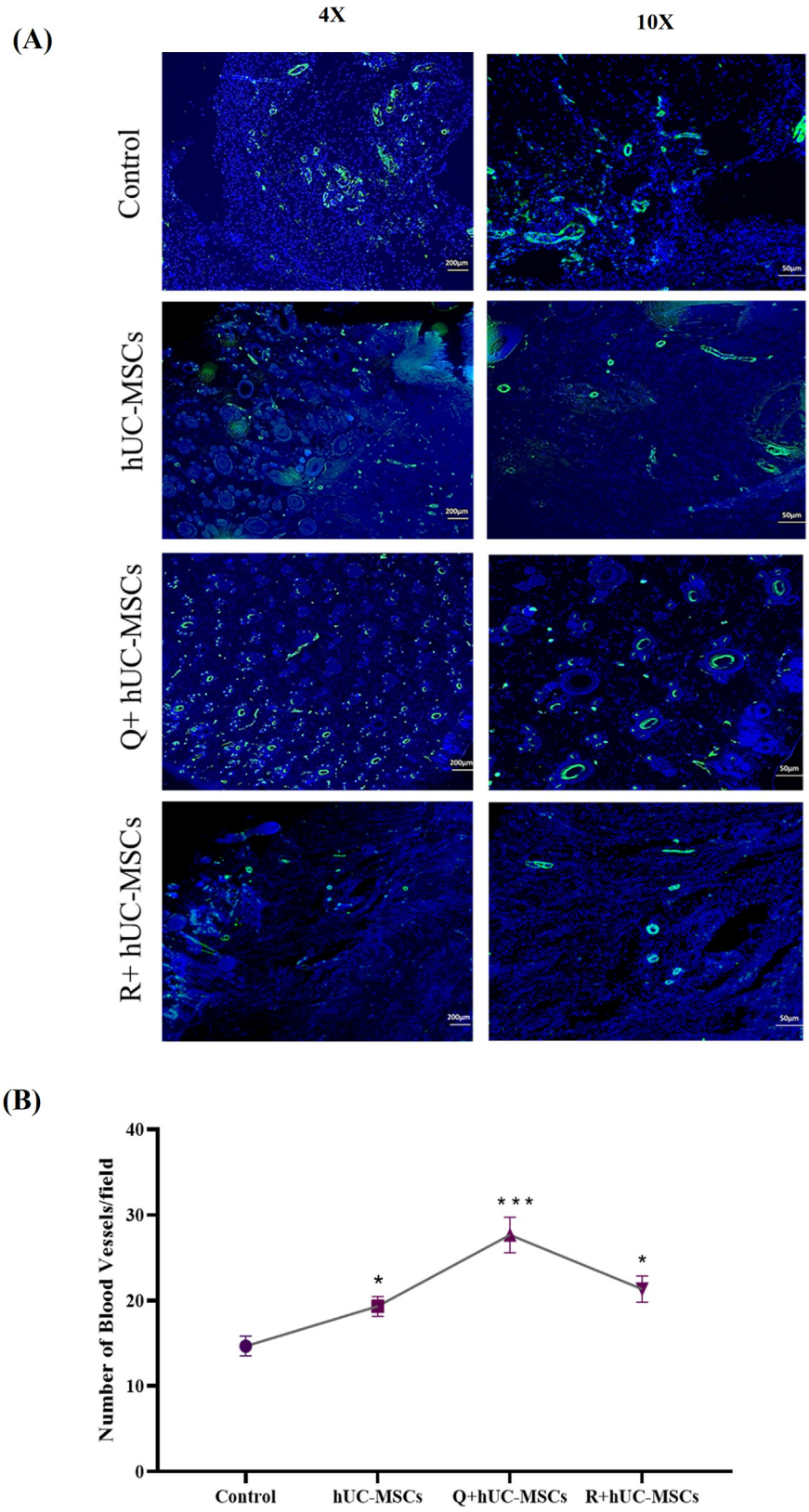

Fig. 6. Immunohistochemical analysis of neo-vascularization (A) Mature blood vessels of different diameters were observed via α-SMA staining at day 14. Images were taken under 4X and 10× magnifications (B) The quantification of blood vessels demonstrated significant increase in the treatment groups with highest number in the Q + hUC-MSC group. For statistical analysis, one-way ANOVA with Bonferroni post-hoc test was performed. Data is represented as mean ± S.E.M (n = 3); p-value ≤ 0.05 was considered statistically significant (where *** = $p < 0.001$, * = $p < 0.05$).

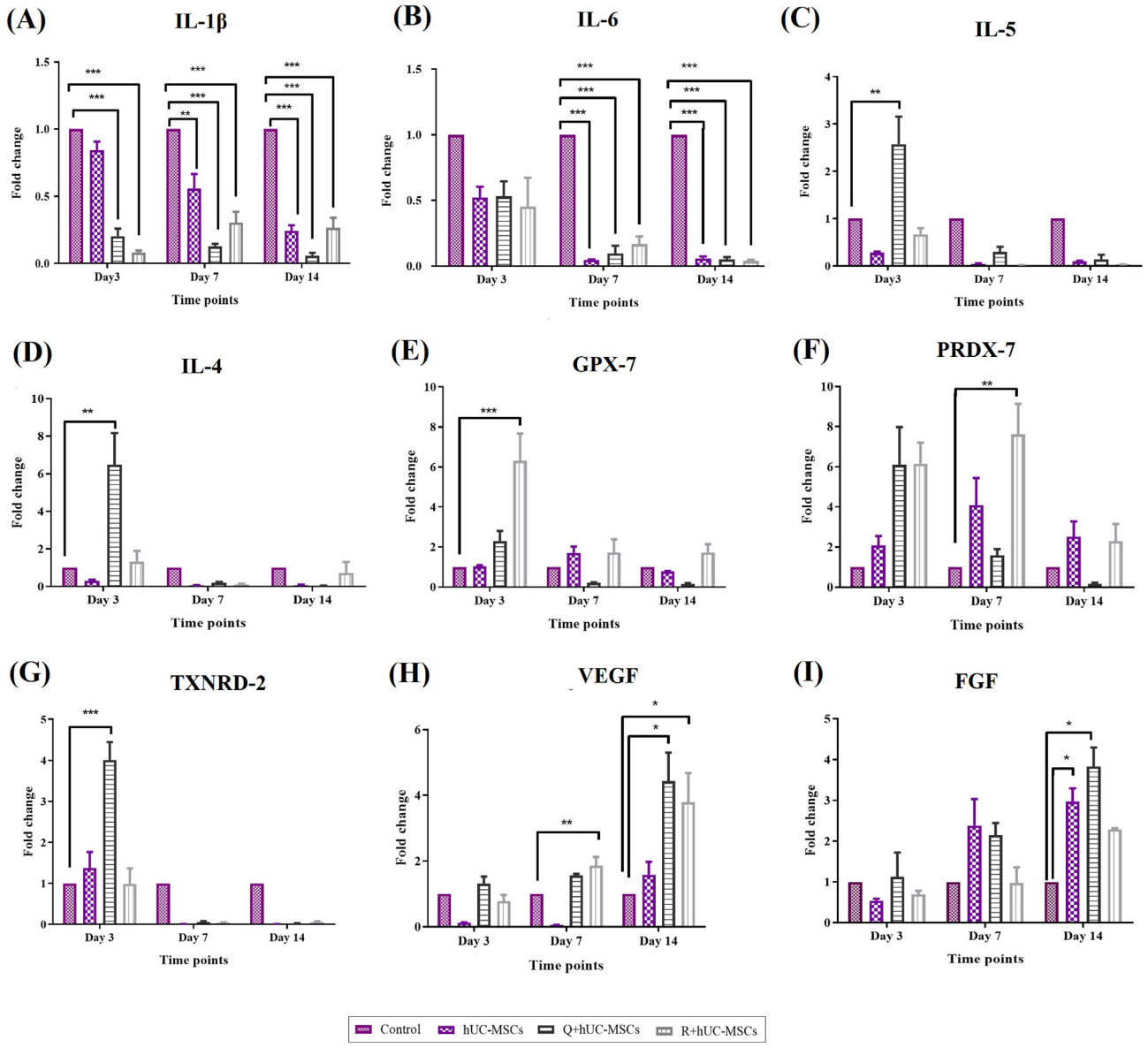

Fig. 7. Gene expression analysis: Gene expression analysis of wound healing cytokines showed that wound healing was significantly improved in the treatment groups as compared to control (A–B) Genes corresponding to inflammatory cytokines, IL-1β and IL-6 showed decreased expression in the treatment groups in contrast to control (C–D) Genes corresponding to anti-inflammatory cytokines, IL-5 and IL-4 (E–G) oxidative stress mediated cytokines, GPX-7, PRDX-7, and TXNRD-2, and (H–I) cell proliferation mediated cytokines, VEGF and FGF showed significant increase in their expression in the treatment groups at days 3, 7 and 14 as compared to control. For statistical analysis, one-way ANOVA with Bonferroni post-hoc test was performed. Data is represented as mean ± S.E.M (n = 3); p-value ≤ 0.05 was considered statistically significant (where *** = $p < 0.001$, ** = $p < 0.01$, * = $p < 0.05$).

MSC group via migration of skin cells as the tissue showed no distortion with reformed compact structure of the dermis. During the later phases of healing, the wound is stabilized by new collagen formation and cell migration towards the peripheries [30]. Our findings showed deposition of squamous epithelial cells at the epidermal peripheries after regeneration in the quercetin and rutin treated hUC-MSC groups. Squamous cell differentiation in the skin tissue shows epidermal maturation, and it also facilitates self-healing without scar formation [31]. Rutin promotes wound healing by proliferation of the collagen fibers, inactivates inflammatory response and promotes cell migration [32]. Quercetin reverses the inflammatory and fibrosis response during healing to protect the skin from the hypertrophic scar and also activates the extracellular remodeling, thus promoting collagen cross linking [15,33].

We observed that recruitment of α-SMA around the blood vessels was increased after treatment of the wound tissue with hUC-MSCs. hUC-MSCs promote angiogenesis which play critical role in granulation tissue formation which indicates maturation of tissue structure [34,35]. Increase in the expression of α-SMA indicates the presence of mature blood vessels; α-SMA helps in contraction and relaxation of blood vessels [36]. A major hallmark of the non-healing wound is the disruption in the process of angiogenesis. In our study, the increase in the number of blood vessels in the treated groups especially Q + hUC-MSC group, ensures enhanced neo-vascularization and angiogenesis. Higher expression of α-SMA indicates improved wound healing through decreased inflammation and enhanced wound closure [37].

Gene expression analysis of wound healing cytokines further confirms the findings of macroscopic and microscopic analyses. Inflammatory, anti-inflammatory, anti-oxidant and remodeling cytokines were quantified at the inflammation (day 3), proliferative (day 7) and remodeling (day 14) phases of wound healing. Our findings showed that preconditioning of hUC-MSCs with quercetin significantly decreased IL-1β and IL-6 and increased IL-5, IL-4, TXNR-2, VEGF, and FGF expression. Rutin preconditioning showed significant decrease in IL-1β and IL-6 and increase in GPX-7, PRDX-7 and VEGF levels. In a previous study, it was reported that IL-1β and IL-6 levels are signs of chronic inflammation and non-healing wounds [38]. Decrease in the levels of inflammatory cytokines, while upregulation of anti-inflammatory cytokines in the quercetin and rutin treatment groups may promote wound healing. Inflammatory cells at the burn site produce reactive oxygen species which cause oxidative damage to cells [39]. The anti-oxidant defense mechanism is essential to adequately progress the wound towards healing [40]. In this study, we analyzed three cytokines that play an important role in scavenging free radicals and reducing oxidative stress i.e., GPX-7, PRDX-7 and TXNR2. PRDX and GPX detoxify peroxidases to avoid generation of harmful hydroxyl radicals [40,41], while TXNR is involved in the intracellular processes and protects against oxidative stress which ultimately reduces inflammation and disease progression [1]. We also observed that growth factors responsible for cell proliferation VEGF and FGF were upregulated at the time period corresponding to remodeling phase. Increased expression of VEGF indicates neovascularization process which starts with proliferation of the endothelial cells to form new vessels [42]. Furthermore, upsurge in the FGF expression represents accelerated granulation, epithelization and angiogenesis, resulting in enhanced wound healing [43].

Recent advancements in the field of stem cell biology have increased the hope of achieving the definitive treatment for regenerative diseases which are considered incurable, such as diabetic foot ulcers, pressure ulcers, and other chronic long-standing conditions. It is important to understand the basic concepts of stem cell biology to utilize this technique effectively. Also, strategies to improve stem cell potential, e.g. preconditioning and tissue engineering approaches should be well understood. Results obtained from this study can be utilized for future clinical application of not only burn wounds, but degenerative pathologies.

5. Conclusion

The study concludes that wound healing potential of hUC-MSCs is enhanced after treatment with quercetin and rutin, the two bioactive compounds of *M. azedarach*. Quercetin was found to be more potent to progress the wound healing towards tissue regeneration. The study revealed that preconditioned hUC-MSCs restored tissue integrity, and promoted epithelialization and regeneration, with no scar formation. Quercetin and rutin possess anti-oxidant and anti-inflammatory properties that aid in enhancing the wound healing efficiency of hUC-MSCs. This study would provide a useful guide towards a better cell based therapy for cold burn wounds using the preconditioned approach.

Declaration of competing interest

The authors declare no conflict of interest.

Ackowledegment

This project is financially supported by National Research Program for Universities (NRPU-HEC) project under the grant number 20-17590. We also acknowledge Zainab Panjwani Memorial Hospitals for providing us the human umbilical cord samples.

References

[1] Reinke JM, Sorg H. Wound repair and regeneration. Eur Surg Res 2012;49(1):35–43. https://doi.org/10.1159/000339613. PMID: 22797712.
[2] Honari G. Skin structure and function. Sensitive skin syndrome. CRC Press; 2017. p. 16–22. https://doi.org/10.1201/9781315121048.
[3] Ahn HN, Kang HS, Park SJ, Park MH, Chun W, Cho E. Safety and efficacy of basic fibroblast growth factors for deep second–degree burn patients. Burns 2010;46(8):1857–66. https://doi.org/10.1016/j.burns.2020.06.019. PMID: 33054995.
[4] O'Connor M, Wang JV, Gaspari AA. Cold burn injury after treatment at whole-body cryotherapy facility. JAAD Case Reports 2019;5(1):29–30. https://doi.org/10.1016/j.jdcr.2018.10.006. PMID: 30555881.
[5] Rathjen NA, Shahbodaghi SD, Brown JA. Hypothermia and cold weather injuries. Am Fam Physician 2019;100(11):680–6. https://doi.org/1201/p680.htmlPMID: 31790182.
[6] Lindholm C, Searle R. Wound management for the 21st century: combining effectiveness and efficiency. Int Wound J 2016;13(2):5–15. https://doi.org/10.1111/iwj.12623 PMID: 27460943.
[7] Dasari N, Jiang A, Skochdopole A, Chung J, Reece E, Vorstenbosch J, et al. Updates in diabetic wound healing, inflammation, and scarring. Semin Plast Surg 2021;35(3):153–8. https://doi.org/10.1055/s-0041-1731460. PMID: 34526862.
[8] Popa LG, Giurcaneanu C, Mihai MM, Beiu C, Orzan OA, Negoita S, et al. The use of cadaveric skin allografts in the management of extensive wounds. Rom J Leg Med 2021;29(1):37–44. https://doi.org/10.4323/rjlm.2021.37.
[9] Doi H, Kitajima Y, Luo L, Yan C, Tateishi S, Ono Y, et al. Potency of umbilical cord blood-and Wharton's jelly-derived mesenchymal stem cells for scarless wound healing. Sci Rep 2016;6(1):1–10. https://doi.org/10.1038/srep18844 PMID: 26728342.
[10] Choi Y, Yoon DS, Lee KM, Choi SM, Lee MH, Park KH, et al. Enhancement of mesenchymal stem cell-driven bone regeneration by resveratrol-mediated SOX2 regulation. Aging and Disease 2019;10(4):818–33. https://doi.org/10.14336/AD.2018.0802 PMID: 31440387.
[11] Aslam MS, Ahmad MS, Riaz H, Raza SA, Hussain S, Qureshi OS, et al. Role of flavonoids as wound healing agent. Phytochemicals-source of Antioxidants and Role in Disease Prevention 2018:95–102. https://doi.org/10.5772/intechopen.79179.
[12] Munir T, Mohyuddin A, Khan Z, Haq R. Exploration of antibacterial potential of Melia azedarach L. Scientific Inquiry and Review 2017;1(1):19–26. https://doi.org/10.29145/sir/11/010103.
[13] M'rabet Y, Rokbeni N, Cluzet S, Boulila A, Richard T, Krisa S, et al. Profiling of phenolic compounds and antioxidant activity of Melia azedarach L. leaves and fruits at two stages of maturity. Ind Crop Prod 2017;107:232–43. https://doi.org/10.1016/j.indcrop.2017.05.048.
[14] Nuutila K, Samandari M, Endo Y, Zhang Y, Quint J, Schmidt TA, et al. In vivo printing of growth factor-eluting adhesive scaffolds improves wound healing. Bioact Mater 2022;8:296–308. https://doi.org/10.1016/j.bioactmat.2021.06.030. PMID: 34541402.
[15] Polerà N, Badolato M, Perri F, Carullo G, Aiello F. Quercetin and its natural sources in wound healing management. Curr Med Chem 2019;26(31):5825–48. https://doi.org/10.2174/0929867325666180713150626 PMID: 30009700.
[16] Jaafar NS, Hamad MN, Abbas IS, Jaafar IS. Qualitative phytochemical comparison between flavonoids and phenolic acids contents of leaves and fruits of *Melia azedarach* (family: meliaceae) cultivated in Iraq by HPLC and HPTLC. Int J Pharm Pharmaceut Sci 2016;8(10):242–50. https://doi.org/10.22159/ijpps.2016v8i10.13868.
[17] Aslam S, Khan I, Jameel F, Zaidi MB, Salim A. Umbilical cord-derived mesenchymal stem cells preconditioned with isorhamnetin: potential therapy for burn wounds. World J Stem Cell 2020;12(12):1652–66. https://doi.org/10.4252/wjsc.v12.i12.1652 PMID: 33505606.
[18] Pinto BI, Cruz ND, Lujan OR, Propper CR, Kellar RS. In vitro scratch assay to demonstrate effects of arsenic on skin cell migration. JoVE 2019;144:e58838. https://doi.org/10.3791/58838. PMID: 30855562.
[19] Benichou G, Yamada Y, Yun SH, Lin C, Fray M, Tocco G. Immune recognition and rejection of allogeneic skin grafts. Immunotherapy 2011;3(6):757–70. https://doi: 10.2217/imt.11.2 PMID: 21668313.
[20] Alrubaiy L, Al-Rubaiy KK. Skin substitutes: a brief review of types and clinical applications. Oman Med J 2009;24(1):4. https://doi: 10.5001/omj.2009.2 PMID: 22303500.
[21] Wang M, Xu X, Lei X, Tan J, Xie H. Mesenchymal stem cell-based therapy for burn wound healing. Burns & Trauma 2021;9:1–15. https://doi: 10.1093/burnst/tkab002 PMID: 34212055.
[22] Lodi D, Iannitti T, Palmieri B. Stem cells in clinical practice: applications and warnings. J Exp Clin Cancer Res 2011;30(1):1–20. https://doi: 10.1186/1756-9966-30-9 PMID: 21241480.
[23] Herrmann JL, Wang Y, Abarbanell AM, Weil BR, Tan J, Meldrum DR. Preconditioning mesenchymal stem cells with transforming growth factor-alpha improves mesenchymal stem cell-mediated cardioprotection. Shock 2010;33(1):24–30. 10.1097/SHK.0b013e3181b7d137 PMID: 19996917.

[24] Chupeco JPM, Flores MLS, Reyes MF. Macroscopic and Microscopic changes in the wound after intradermal closure using buried knot and pulley knot-free patterns following ovariectomy in cats. Philipp J Vet Anim Sci 2014;39(2):277–86. https://doi.org/10.1.1.877.1389.
[25] Liesveld JL, Sharma N, Aljitawi OS. Stem cell homing: from physiology to therapeutics. Stem Cell 2020;38(10):1241–53. https://doi.org/10.1002/stem.3242 PMID: 32526037.
[26] Hocking AM. The role of chemokines in mesenchymal stem cell homing to wounds. Adv Wound Care 2015;4(11):623–30. https://doi.org/10.1089/wound.2014.0579. PMID: 26543676.
[27] Yeum CE, Park EY, Lee SB, Chun HJ, Chae GT. Quantification of MSCs involved in wound healing: use of SIS to transfer MSCs to wound site and quantification of MSCs involved in skin wound healing. Journal of Tissue Engineering and Regenerative Medicine 2013;7(4):279–91. https://doi.org/10.52547/ibj.25.5.334 PMID: 22278819.
[28] Cheng KY, Lin ZH, Cheng YP, Chiu HY, Yeh NL, Wu TK, et al. Wound healing in streptozotocin-induced diabetic rats using atmospheric-pressure argon plasma jet. Sci Rep 2018;8(1):1–15. https://doi.org/10.1038/s41598-018-30597-1. PMID: 30111887.
[29] Gopalakrishnan A, Ram M, Kumawat S, Tandan SK, Kumar D. Quercetin accelerated cutaneous wound healing in rats by increasing levels of VEGF and TGF-β1. Indian J Exp Biol 2016;54(1):187–95. https://doi.org/10.1080/08977194.2020.1822830 PMID: 27145632.
[30] Moore AL, Marshall CD, Barnes LA, Murphy MP, Ransom RC, Longaker MT. Scarless wound healing: transitioning from fetal research to regenerative healing. Wiley Interdisciplinary Reviews: Dev Biol 2018;7(2):1–37. https://doi.org/10.1002/wdev.309 PMID: 29316315.
[31] Alarcon-Martinez L, Yilmaz-Ozcan S, Yemisci M, Schallek J, Kılıç K, Can A, et al. Capillary pericytes express α-smooth muscle actin, which requires prevention of filamentous-actin depolymerization for detection. Elife 2018;7:1–17. https://doi.org/10.7554/eLife.34861. PMID: 29316315.
[32] Chen LY, Huang CN, Liao CK, Chang HM, Kuan YH, Tseng TJ, et al. Effects of rutin on wound healing in hyperglycemic rats. Antioxidants 2020;9(11):1122–8. https://doi.org/10.3390/antiox9111122 PMID: 33202817.
[33] Jangde R, Srivastava S, Singh MR, Singh D. *In vitro* and *In vivo* characterization of quercetin loaded multiphase hydrogel for wound healing application. Int J Biol Macromol 2018;115:1211–7. https://doi.org/10.1016/j.ijbiomac.2018.05.010 PMID: 29730004.
[34] Zhang J, Guan J, Niu X, Hu G, Guo S, Li Q, et al. Exosomes released from human induced pluripotent stem cells-derived MSCs facilitate cutaneous wound healing by promoting collagen synthesis and angiogenesis. J Transl Med 2015;13(1):1–14. https://doi.org/10.1186/s12967-015-0417-0. PMID: 25638205.
[35] Jiang D, Qi Y, Walker NG, Sindrilaru A, Hainzl A, Wlaschek M, et al. The effect of adipose tissue derived MSCs delivered by a chemically defined carrier on full-thickness cutaneous wound healing. Biomaterials 2013;34(10):2501–15. https://doi.org/10.1016/j.biomaterials.2012.12.014. PMID: 23317813.
[36] Luo M, Wang M, Niu W, Chen M, Cheng W, Zhang L, et al. Injectable self-healing anti-inflammatory europium oxide-based dressing with high angiogenesis for improving wound healing and skin regeneration. Chem Eng J 2021;412:128471. https://doi.org/10.1016/j.cej.2021.128471.
[37] Krzyszczyk P, Schloss R, Palmer A, Berthiaume F. The role of macrophages in acute and chronic wound healing and interventions to promote pro-wound healing phenotypes. Front Physiol 2018;9:419–26. https://doi.org/10.3389/fphys.2018.00419. PMID: 29765329.
[38] Parihar A, Parihar MS, Milner S, Bhat S. Oxidative stress and anti-oxidative mobilization in burn injury. Burns 2008;34(1):6–17. https://doi.org/10.1016/j.burns.2007.04.009. PMID: 17905515.
[39] Mittal M, Siddiqui MR, Tran K, Reddy SP, Malik AB. Reactive oxygen species in inflammation and tissue injury. Antioxidants Redox Signal 2014;20(7):1126–67. https://doi.org/10.1089/ars.2012.5149. PMID: 23991888.
[40] Kurahashi T, Fujii J. Roles of antioxidative enzymes in wound healing. J Dev Biol 2015;3(2):57–70. https://doi.org/10.3390/jdb3020057.
[41] Kiafar B, Binabaj MM, Jafarian AH, Khazan Z, Hashemy SI. The relationship between tissue thioredoxin reductase activity and the psoriasis area and severity index. Indian J Dermatol 2020;65(1):29–32. https://doi.org/10.4103/ijd.IJD_327_18. PMID: 32029936.
[42] Wahl EA, Schenck TL, Machens HG, Balmayor ER. VEGF released by deferoxamine preconditioned mesenchymal stem cells seeded on collagen-GAG substrates enhances neovascularization. Sci Rep 2016;6(1):1–12. https://doi.org/10.1155/2021/6676609 PMID: 27830734.
[43] Nishino Y, Ebisawa K, Yamada Y, Okabe K, Kamei Y, Ueda M. Human deciduous teeth dental pulp cells with basic fibroblast growth factor enhance wound healing of skin defect. J Craniofac Surg 2011;22(2):438–42. https://doi.org/10.1097/SCS.0b013e318207b507. PMID: 21403563.